Cluster Expansion for Solid Orthohydrogen†

R. J. Lee
Department of Physics, Purdue University Fort Wayne Campus, Fort Wayne, Indiana 46805*
and Institute for Atomic Research and Department of Physics, Iowa State University, Ames, Iowa 50010‡
and
J. C. Raich
Department of Physics, Colorado State University, Fort Collins, Colorado 80521
(Received 7 September 1971)

The cluster variation method previously applied to calculate the thermal behavior of ferro- and antiferromagnets near the Curie temperature is extended to a discussion of solid hydrogen near its order-disorder transition. An attempt is made to describe the relationship between the order-disorder transition and the crystallographic phase change. The orientational free energies of the orthohydrogen or paradeuterium systems are calculated for both the face-centered cubic (fcc) and the hexagonal close-packed (hcp) lattices. The space group $Pa3$ is assumed for the fcc case and $Pca2_1$ for the hcp case. Within the cluster variation approximation, a first-order transition is found to occur when the free energies for the fcc and hcp phases cross. The fcc-hcp crystallographic transition occurs near the onset of the orientational ordering in the cubic phase. This prediction is in good agreement with experiment except when repeated cycling is performed.

I. INTRODUCTION

Numerous theoretical and experimental studies of the phase transition in solid hydrogen and deuterium have been made in the past few years. For a review of recent experimental and theoretical work, the reader is referred to Refs. 1–19. Although both crystallographic and orientational order-disorder transitions are believed to occur, the main theoretical effort has been directed toward an understanding of the cooperative ordering of orthohydrogen (o-H_2) or paradeuterium (p-D_2) molecules on rigid face-centered cubic (fcc) and hexagonal close-packed (hcp) lattices.[1–12] It has been shown that the dominant contribution to the anisotropic interactions is an electrostatic-quadrupole-quadrupole (EQQ) coupling and also that the EQQ interactions lead to an orientational ordering of the molecules below some critical temperature in a manner similar to the ordering of spins in an antiferromagnet. Since the EQQ interactions can be represented in a form rather analogous to the Ising and Heisenberg models of magnetism, the previous calculations[2–12] have made use of a number of techniques developed in the theories of magnetic phase transitions.

Molecular-field calculations,[1–4] spin-wave treatments,[5–9] a higher-order Bethe calculation,[13] and an exact model[14] all predict an orientational ordering of the o-H_2 molecules, although they do not give good descriptions of the transition region. The molecular-field and spin-wave treatments predict first-order transitions, the Bethe approximation and the exact model more gradual transitions. Also, all theories overestimate the transition temperature by about a factor of 2. The molecular-field and spin-wave treatments consider only the effects of long-range order and are essentially low-temperature theories. These treatments would give an accurate description of the transition region only if the effects of the short-range correlations between molecules on the free energy were negligible. The Bethe model and the exact theory mentioned above start with a truncated Hamiltonian with no off-diagonal terms.

High-temperature expansions[15,16] include short-range correlations *only*. These expansions are strictly valid for temperatures considerably above the transition region. Raich and Etters[15] extrapolate their high-temperature results into the transition region to point out that the low-temperature theories cannot give an accurate description of the transition region in o-H_2. They find that the low-temperature theories significantly underestimate the effects of the short-range correlations. In fact, the molecular-field term contributes only about one-half of the total orientational free energy in the transition region. Apparently the nature of the EQQ interactions make the contributions of the short-range correlations between molecules to the free energy important. This can be understood by realizing the lowest-energy configuration for a pair alone is different than the zero-temperature pair configuration in the crystal. Therefore, one would expect the competition between these two configurations to result in a considerable rearrangement of the molecules as the temperature is increased and the long-range correlations decrease.

An alternative description is one which starts from a spin-wave model of the librational motion of the molecules in the crystal.[5–9] The relative instability of the low-temperature structure, $Pa3$ for the fcc case, manifests itself through the large

anharmonic contributions to the spin-wave Hamiltonian.[10]

Recent experiments indicate that the hcp-fcc crystallographic and orientational order-disorder transitions do not occur simultaneously, but that the orientational transition is responsible for the crystallographic transition.[18-20] Also, calculations by Nosanow[21] indicate the difference in zero-point lattice energies for the hcp and fcc crystals may not be enough to stabilize one over the other, at least when orientational forces are important. Since the structural and orientational transitions are closely related, it is of interest to compare the free energies of the hcp and fcc crystals in an effort to understand their connection. The effects of the short-range correlations on the free energy are expected to be signiiicant in the transition region, and therefore, it is important to include them in such a calculation.

The purpose of this paper is threefold: (i) Develop a variational cluster approximation for the free energy of a system of o-H_2 (or p-D_2) molecules with EQQ interactions which includes to some extent both long-range and short-range correlations; (ii) apply the cluster approximation to examine the effects of the short-range order on the orientational ordering in the transition region; and (iii) examine the effect of the EQQ interactions on the hcp-fcc structural transition.

In this paper we have only considered the librational motions of the molecules. The translational phonon contribution, as well as the associated static lattice energy were not considered. A complete discussion of the observed transition must include both librational and translational modes.[22,23] For convenience we discuss only the case of o-H_2. The results for p-D_2 are qualitatively the same.

A model of o-H_2 molecules coupled by an EQQ potential on rigid hcp and fcc lattices is discussed in Sec. II. The cluster expansion of Strieb, Callen, and Horwitz[24] (hereafter referred to as SCH) is applied to the case of solid o-H_2 in Sec. III. The numerical calculations are outlined in Sec. IV, Sec. V contains the results, and Sec. VI the conclusions.

II. MODEL

The model used here has been extensively described in the literature.[2] It consists of a system of H_2 molecules in the rotational angular momentum state $J=1$ on a rigid lattice interacting via EQQ forces. The separation of successive rotational energy levels of the H_2 molecule is equal to 593 cm^{-1} and the orientational coupling energy varies by less than 30 cm^{-1}. This implies that the EQQ interaction is a small perturbation on the rotational levels, and therefore J remains almost a good quantum number in the lattice. As a result, it is a good approximation at low temperatures to treat a system of o-H_2 molecules as all being in the rotational state $J=1$.

A. Hamiltonian

As previously discussed, the main anisotropic contribution to the intermolecular interactions are the EQQ interactions.[16] The EQQ Hamiltonian is

$$H=\tfrac{1}{2}\sum_{ij} V_{ij}(\vec{\Omega}_i, \vec{\Omega}_j, \vec{\Omega}_{ij}), \tag{2.1}$$

where $\vec{\Omega}_i=(\theta_i, \phi_i)$ specifies the orientation of a molecule on site i relative to the crystal axis. The term V_{ij} represents the EQQ interaction between molecules i and j and can be written[25]

$$V_{ij}=\frac{20\pi}{9}(70\pi)^{1/2}\Gamma_{ij}\sum_{MN} C(224;MN) \times Y_{2M}(\vec{\Omega}_i)\, Y^*_{4,M+N}(\vec{\Omega}_{ij}). \tag{2.2}$$

Here $C(J_1J_2J;M_1M_2)$ is a Clebsch-Gordan coefficient,[26] $\Gamma_{ij}=6e^2Q^2/25R_{ij}^5$, where Q is the molecular quadrupole moment,[2] $\vec{R}_{ij}$ is the vector connecting sites i and j measured relative to the crystal axis, and the $Y_{lm}(\theta_i, \phi_i)$ are spherical harmonics.

The two lattices considered here both have four sublattices with the molecular equilibrium directions along the axes of quantization for each molecule. It is therefore convenient to transform to a coordinate system where the z_i axis for each molecule i is along the symmetry direction for that molecule.[7] This transformation is[26]

$$Y_{2M}(\vec{\Omega}_i)=\sum_m D^2_{Mm}(\alpha_i, \beta_i, \gamma_i)^*\, Y_{2m}(\vec{\omega}_i). \tag{2.3}$$

Here D^2_{Mm} is a rotation matrix, α_i, β_i, γ_i are the Euler angles which specify the orientation of the z_i axis relative to the crystal axis, and $\vec{\omega}_i=(\theta_i, \phi_i)$ specifies the orientation of the molecule at i relative to its equilibrium axis.

In the subspace of $J=1$, one can replace the spherical harmonics by their operator equivalents[16]

$$Y_{2m}(\vec{\omega}_i)=A_m O_i^m, \tag{2.4}$$

where

$$A_0=-\tfrac{1}{5}(5/4\pi)^{1/2}, \quad A_{\pm1}=\pm\tfrac{1}{10}(15/2\pi)^{1/2}, \quad A_{\pm2}=\tfrac{1}{10}(15/2\pi)^{1/2}, \tag{2.5}$$

and

$$O_i^0=3(J_i^z)^2-2, \quad O_i^{\pm1}=J_i^zJ_i^\pm+J_i^\pm J_i^z, \quad O_i^{\pm2}=(J_i^\pm)^2. \tag{2.6}$$

Here $J_i^\pm=J_i^x\pm iJ_i^y$, where J_i^x, J_i^y, J_i^z are the components of the rotational angular momentum $\vec{J}$. O_i^m operates on the states $|J_i, M_i\rangle=|1, M_i\rangle=|M_i\rangle$, where M_i is the quantum number of J_i^z. The Ham-

iltonian can now be written in operator form

$$H=\sum_{ij}\sum_{mn}\gamma_{ij}^{mn}O_i^m O_j^n, \tag{2.7}$$

where

$$\gamma_{ij}^{mn}=\frac{10\pi}{9}(70\pi)^{1/2}\Gamma_{ij}A_m A_n\sum_{MN}C(224;MN)\times Y_{M+N}^{*}(\vec{\Omega}_{ij})\,D_{Mm}^{2*}(\alpha_i,\beta_i,\gamma_i)\,D_{Nn}^{2*}(\alpha_j,\beta_j,\gamma_j).$$

B. Molecular Structures

In order to illustrate the application of the cluster variation method we limit ourselves to only two structures: fcc with a Pa3 space group and hcp with a space group $Pca2_1$. The Pa3 space group for the fcc lattice is indicated by studies of arrays of classical quadrupoles.[27,28] James and Raich[2] found the $Pa3$ structure yields a self-consistent description of the ordered state of a system of interacting H_2 molecules coupled by EQQ forces. This space group is also consistent with x-ray, neutron, infrared, Raman data, and $(\partial p/\partial T)_V$ measurements.[18–20,29–32] Initial Raman scattering experiments found lines in the libron spectra which seemed to be inconsistent with the $Pa3$ structure.[30] This discrepancy has been resolved by Harris who finds that consideration of libron-libron interactions yields theoretical Raman lines which are in good agreement with experiment.[10]

The high-temperature phase is known to be hcp. Except possibly very near the transition temperature, no long-range ordering of the molecular orientations seems to occur in the hcp phase. A systematic study by Miyagi and Nakumura of possible configurations for the ordered ($T=0$) ground state of hcp o-H_2 concluded that a $Pca2_1$ space group minimized the ground-state energy.[33] Computer calculations by James[34] confirmed this conclusion for $T=0$, but that the equilibrium orientations are temperature dependent and that other hexagonal space groups may be favored at higher temperatures. The present calculation assumes a $Pca2_1$ space group for the hcp phase at all temperatures, neglecting any temperature dependence of the equilibrium orientations. Although it is found that the molecules are not ordered in the long-range order sense in the hcp phase at high temperatures, the assumption of certain equilibrium orientations is necessary for the application of the cluster variation approximation. The actual molecular orientations at high temperatures will differ considerably from the assumed long-range ordered structure. In fact, in the high-temperature limit the results of the cluster variation method starting from any particular long-range orientational configuration are independent of that configuration and must reduce to the usual high-temperature expansions.[16,17] We have allowed for the possibility of a nonideal c/a ratio. The volume per molecule is held constant when the c/a ratio is varied. The fcc and hcp volumes were taken to be equal although a small volume change at the transition has been measured.[32] Such a volume change can only be discussed if a nonrigid lattice model is considered.

The $Pa3$ and $Pca2_1$ lattices both have four sublattices with all the molecules on a particular sublattice having the same equilibrium orientations. Figures 1 and 2 show the $Pa3$ and $Pca2_1$ structures; Tables I and II give the orientations of the equlibrium axes and intermolecular directions with respect to the crystal axis. These are used in the calculation of the γ_{ij}^{mn} defined in Sec. II A for the two lattices.

III. CLUSTER EXPANSION

Preliminary discussions of the application of the cluster variation method to the ordering of molecules in solid hydrogen and deuterium have been given by the authors.[35,36] In order to perform the cluster expansion, the Hamiltonian is separated into perturbed and unperturbed parts.[24] This is done by introducing an expansion parameter $\bar{O}$ and an operator α_i which represents the deviation of O_i^0 from $\bar{O}$. The "best" value of $\bar{O}$ is to be determined by minimizing the free energy with respect to it. It is to be noted that $\bar{O}$ will not in general turn out to be $\langle O_i^0\rangle$. This is only the case for the zeroth-order expression. For higher-order clusters, $\bar{O}$ plays the role of an "effective" field parameter acting on the cluster.

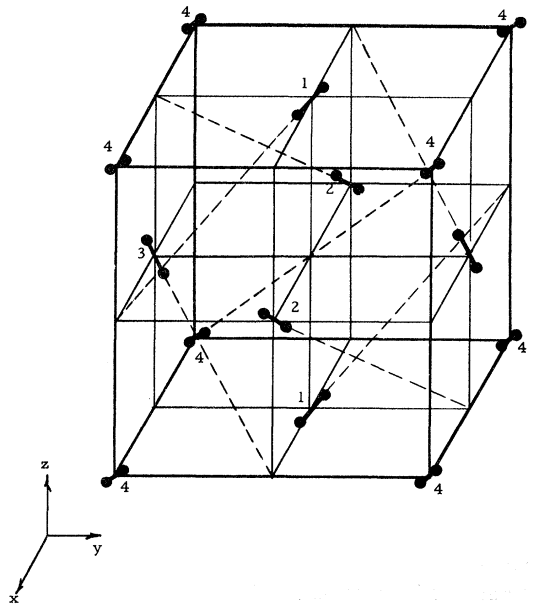

FIG. 1. Orientations of the symmetry axes of the molecular ground states of H_2 molecules on an fcc lattice. The numbers show the sublattice to which each molecule belongs. $Pa3$ space group.

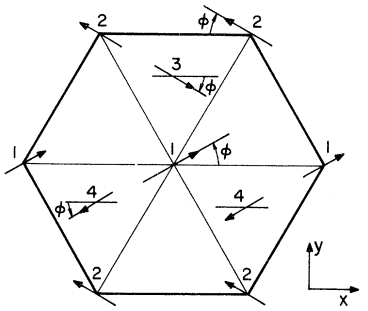

FIG. 2. Orientations of the symmetry axes of the molecular ground states of H_2 molecules on a hcp lattice. The numbers show the sublattice to which each molecule belongs. Arrows at vertices represent molecules in one hexagonal plane, arrows at the center of triangles represent molecules in the hexagonal planes immediately above or below. The arrowhead indicates the end of the molecule that lies above the hexagonal plane. All symmetry axes make an angle of 55° with the z axis and ϕ equals 43.5°. $Pca2_1$ space group.

After adding and subtracting $\sum_{ij}\gamma_{ij}^{00}O_i^0O_j^0$ to (2.7), and rewriting the Hamiltonian in terms of α_i, the Hamiltonian can be written

$$H = H_0 + H' \ . \tag{3.1}$$

Here

$$H_0 = E_0 + \xi\sum_i \alpha_i \ , \tag{3.2}$$

where

$$E_0 = N\gamma(0)\,\bar{O}^2 \ ,$$
$$\xi = -2\gamma(0)\,\bar{O} \ , \tag{3.3}$$
$$\alpha_i = \bar{O} - O_i^0 \ ,$$

and

$$H' = \sum_{ij}(\gamma_{ij}^{00}\alpha_i\alpha_j + \sum_{mn}\gamma_{ij}^{mn}O_i^mO_j^n - \gamma_{ij}^{00}O_i^0O_j^0) \ . \tag{3.4}$$

In the above,

$$\gamma(0) = \sum_j \gamma_{ij}^{00} = \sum_{j=1}^{z}\gamma_{ij}^{00} \tag{3.5}$$

for the case of nearest-neighbor interactions. Here z equals the number of nearest neighbors.

A. Zeroth Order

The unperturbed free energy F_0 is now defined

$$-\beta F_0 = \ln \mathrm{Tr}e^{-\beta H_0} \ , \tag{3.6}$$

and the correction is

$$-\beta F' = -\beta F + \beta F_0 = \ln \mathrm{Tr}e^{-\beta H} - \ln \mathrm{Tr}e^{-\beta H_0} \ . \tag{3.7}$$

The unperturbed portion can be easily evaluated to give

$$-\beta F_0 = N\gamma(0)\,\bar{O}^2 + N\ln\Phi \ , \tag{3.8}$$

where

$$\Phi = \mathrm{Tr}e^{+\beta\xi O_i^0} \ . \tag{3.9}$$

The trace in (3.9) is over the states $M_i = \pm 1$, 0 and

$$O_i^0|M_i\rangle = [3(M_i)^2 - 2]|M_i\rangle \ . \tag{3.10}$$

B. Cluster Expansion of F'

We define the operator V by the equation

$$e^{-\beta(H_0+H')} = e^{-\beta H_0}e^{-\beta V} \ . \tag{3.11}$$

It has been shown by Blinc and Svetina[37] that

$$V = H' + (\beta/2!)[H_0, H'] + (\beta^2/3!)[H_0,[H_0,H']] + \cdots \ . \tag{3.12}$$

[Note that for the case of ferromagnetism, H_0 commutes with H' and so the separation of $e^{-\beta(H_0+H')}$ can be made without using (3.12). Also, the equations developed below for the expansion of F' become identical to those of SCH if one sets $Q'_\alpha = Q_\alpha$, as shown below.] With this, the perturbation part of the free energy becomes

$$-\beta F' = \ln\left(\frac{\mathrm{Tr}\,e^{-\beta H_0}e^{-\beta V}}{\mathrm{Tr}\,e^{-\beta H_0}}\right) = \ln \mathrm{Tr}\rho_0 e^{-\beta V} = \ln\langle e^{-\beta V}\rangle \ . \tag{3.13}$$

Here the average is defined with respect to the unperturbed density matrix

TABLE I. Orientations of molecules and intermolecular axes in fcc o-H_2. $Pa3$ space group. $a = \sqrt{2}\times 3.757$ Å $= \sqrt{2}\times$ lattice constant.

Sublattices	Coordinates with respect to cube corner	Direct cosines γ of equilibrium axes of molecules on sublattice	Polar angles specifying the directions $\vec{\Omega}_{ij}$ from a molecule on sublattice 4 to nearest neighbors on sublattices 1, 2, 3
1	$a/2$, $a/2$, 0	$3^{-1/2}(-1, 1, 1)$	$\theta = \pi/2$, $\phi = \pm\pi/4, \pm 3\pi/4$
2	0, $a/2$, $a/2$	$3^{-1/2}(1, -1, 1)$	$\theta = \pi/4$, $3\pi/4$ $\phi = \pi/2$, $3\pi/2$
3	$a/2$, 0, $a/2$	$3^{-1/2}(1, 1, -1)$	$\theta = \pi/4$, $3\pi/4$ $\phi = 0$, π
4	0, 0, 0	$3^{-1/2}(1, 1, 1)$	

TABLE II. Orientations of molecules and intermolecular axes in hcp o-H_2. $Pca2_1$ space group. The length of unit-cell side along the hexagonal axis is c. The nearest-neighbor distance is a for molecules in the same hexagonal plane and r for molecules in different hexagonal planes. For the ideal hcp case where $c/a=(8/3)^{1/2}$, $r=a$, and $c/2r=(2/3)^{1/2}$. $\gamma_1=0.59419$, $\gamma_2=0.56387$, $\gamma_3=0.57385$, $a=3.761$ Å = lattice constant.

Sublattice	Coordinates with respect to center of hexagon	Direction cosines γ of equilibrium axes of molecules on sublattice	Polar angles specifying the directions $\vec{\Omega}_{ij}$ from a molecule on sublattice 1 to nearest neighbors on sublattices 1, 2, 3, 4
1	0, 0, 0	$(\gamma_1, \gamma_2, \gamma_3)$	$\theta=\pi/2$, $\phi=0$, π
2	$a/2$, $\sqrt{3}a/2$, 0	$(-\gamma_1, \gamma_2, \gamma_3)$	$\theta=\pi/2$, $\phi=\pi/3$, $2\pi/3$, $4\pi/3$, $5\pi/3$
3	0, $a/\sqrt{3}$, $c/2$	$(\gamma_1, -\gamma_2, \gamma_3)$	$\theta=\cos^{-1}(\pm c/2r)$, $\phi=\pi/2$
4	$-a/2$, $-a/2\sqrt{3}$, $c/2$	$(-\gamma_1, -\gamma_2, \gamma_3)$	$\theta=\cos^{-1}(\pm c/2r)$ $\phi=7\pi/6$, $11\pi/6$

$$\rho_0 = e^{-\beta H_0}/\mathrm{Tr}e^{-\beta H_0}\,, \tag{3.14}$$

in terms of which the average of an operator A is

$$\langle A\rangle = \mathrm{Tr}\rho_0 A\,. \tag{3.15}$$

H' can be written as

$$H' = \sum_{ij}\tilde{V}_{ij} = 2\sum_{\alpha} Q_\alpha\,, \tag{3.16}$$

where $\alpha=(i,j)$ numbers the pairs or "links" in the crystal. The commutator $[H_0, H']$ again is a sum of two-body interactions:

$$\begin{aligned}[H_0, H'] &= -\xi\sum_{ij}\sum_{l}[O_l^0, \tilde{V}_{ij}]\\ &= 3\xi\sum_{ij}\sum_{\pm}\sum_{mn}\gamma_{ij}^{mn}(J_i^{\pm}O_j^n\delta_{m,\pm1} + O_i^m J_j^{\pm}\delta_{n,\pm1})\\ &= \sum_{ij}V'_{ij} = 2\sum_{\alpha}[H_0, Q_\alpha]\,.\end{aligned} \tag{3.17}$$

Similar expressions are found for higher-order terms. Therefore one can also write V as a sum of pair interactions

$$V = 2\sum_{\alpha} Q'_\alpha\,, \tag{3.18}$$

where

$$\begin{aligned}Q'_\alpha &= Q_\alpha + (\beta/2!)[H_0, Q_\alpha]\\ &\quad + (\beta^2/3!)[H_0,[H_0, Q_\alpha]] + \cdots\,.\end{aligned} \tag{3.19}$$

As a result $-\beta F'$ becomes

$$-\beta F' = \ln\langle e^{-2\beta\sum_\alpha' Q'_\alpha}\rangle\,. \tag{3.20}$$

With the correction to the free energy in this form, the cluster expansion of SCH can be applied to this problem. In that paper, SCH show that for a free energy which can be expressed in terms of pair interactions, a cluster expansion can be performed in terms of clusters of links. After this is done, the expansion can be regrouped so as to apply to clusters of spins, or molecules in the present problem. They arrive at the following expression for F':

$$-\beta F' = \sum_{\{\delta\}}\Big[\sum_{\{\alpha\}_\delta}[-\beta F_{\{\alpha\}_\delta}]\Big] = \sum_{\{\delta\}}[-\beta F_{\{\delta\}}]\,. \tag{3.21}$$

In the above, $\{\delta\}$ is a cluster of spins. $\{\alpha\}_\delta$ designates a set of links which can be drawn among the spins $\{\delta\}$ in such a manner that there exists some path from each spin to every other spin. The contribution to $F_{\{\delta\}}$ of each set of links $\{\alpha\}_\delta$ is given by

$$-\beta F_{\{\alpha\}_\delta} = \sum_{\{\alpha'\}}^{\{\alpha\}_\delta}(-1)^{[\alpha]-[\alpha']}\ln\langle e^{-2\beta\sum_{\alpha'}Q'_{\alpha'}}\rangle\,. \tag{3.22}$$

The sets of links $\{\alpha'\}$ over which the summation is to be carried constitute all subsets of the set $\{\alpha\}_\delta$. $[\alpha]$ and $[\alpha']$ denote the number of links in $\{\delta\}$ and $\{\alpha\}_\delta$, respectively. The $\sum_{\alpha'}$ goes over all links in the set $\{\alpha'\}$.

C. Two-Spin Cluster Approximation

Using (3.21) and (3.22), it is found that the two-spin contribution to the free-energy correction term $(-\beta F')$ is given by

$$-\beta F'_{(2)} = \sum_{(ij)}\ln\langle e^{-2\beta Q'_{ij}}\rangle\,, \tag{3.23}$$

where Q'_{ij} is given by (3.19), and the summation is over all pairs (ij). Considering only nearest-neighbor interactions, and assuming all sites i are equivalent, (3.23) becomes

$$-\beta F'_{(2)} = \frac{N}{2}\sum_{j=1}^{z}\ln\langle e^{-2\beta Q'_{ij}}\rangle\,. \tag{3.24}$$

One must evaluate

$$\ln\langle e^{-2\beta Q'_{ij}}\rangle = \ln\mathrm{Tr}e^{-\beta H_0}e^{-2\beta Q'_{ij}} + \beta F_0\,. \tag{3.25}$$

Since $[H_0,\ Q'_{ij}]\neq 0$, the exponents in (3.25) cannot be added. However, using (3.11) and (3.12) with $H'=2Q'_{ij}$ yields

$$e^{-\beta(H_0+2Q_{ij})} = e^{-\beta H_0}e^{-\beta V}\,, \tag{3.26}$$

with

$$V = 2Q_{ij} + (\beta/2!)[H_0, 2Q_{ij}] + \cdots = 2Q'_{ij}\,. \tag{3.27}$$

Therefore,

$$e^{-\beta(H_0+2Q_{ij})} = e^{-\beta H_0} e^{-2\beta Q'_{ij}} , \tag{3.28}$$

and (3.25) becomes

$$\ln \mathrm{Tr} e^{-\beta(H_0+2Q_{ij})} + \beta F_0 . \tag{3.29}$$

Inserting $\alpha_i = \overline{O} - O_i^0$, Q_{ij} becomes

$$Q_{ij} = \gamma_{ij}^{00}\overline{O}^2 - \gamma_{ij}^{00}\overline{O}\,(O_i^0 + O_j^0) + \sum_{mn} \gamma_{ij}^{mn} O_i^m O_j^n \tag{3.30}$$

and

$$H_0 + 2Q_{ij} = -N\gamma(0)\,\overline{O}^2 + 2\gamma_{ij}^{00}\overline{O}^2 - \xi \sum_{i' \neq i,j} O_i^0 + H_2(ij) , \tag{3.31}$$

where

$$H_2(ij) = 2\left[-(\tfrac{1}{2}\xi + \gamma_{ij}^{00}\overline{O})(O_i^0 + O_j^0) + \sum_{mn} \gamma_{ij}^{mn} O_i^m O_j^n \right]. \tag{3.32}$$

Substituting (3.32) into (3.29), one has

$$\ln\langle e^{-2\beta Q'_{ij}}\rangle = -2\beta\gamma_{ij}^{00}\overline{O}^2 - 2\ln\Phi + \ln \sum_{l=1}^{9} e^{-\beta\nu_l(ij)} , \tag{3.33}$$

where the $\nu_l(ij)$ are the eigenvalues of $H_2(ij)$. With this, $-\beta F'_{(2)}$ becomes

$$-\beta F'_{(2)} = -N\gamma(0)\,\overline{O}^2 - Nz\ln\Phi + \frac{N}{2}\sum_{j=1}^{z} \ln \sum_{l=1}^{9} e^{-\beta\nu_l(ij)} . \tag{3.34}$$

Adding the zeroth-order and the two-spin contributions, one has the complete two-spin cluster approximation to the free energy:

$$-\beta F_2 = -\beta F_0 - \beta F'_{(2)}$$

$$= N(1-z)\ln\Phi + \frac{N}{2}\sum_{j=1}^{z} \ln \sum_{l=1}^{9} e^{-\beta\nu_l(ij)} . \tag{3.35}$$

For the $Pa3$ lattice, all pairs (ij) are equivalent,

$$\gamma_{ij}^{00} = \begin{cases} \gamma^{00} & \text{if } ij \text{ are nearest neighbors} \\ 0 & \text{otherwise} \end{cases}$$

and

$$\gamma(0) = z\gamma^{00} .$$

In this case $\nu_l(ij) = \nu_l$ and (3.33) becomes

$$-\beta F_{(2)} = N(1-z)\ln\Phi + \frac{Nz}{2}\ln\sum_{l=1}^{9} e^{-\beta\nu_l} , \tag{3.36}$$

which is identical to Eq. (52) of SCH. For less symmetric lattices, (3.35) will not necessarily reduce to (3.36). In particular for the $Pca2_1$ lattice, the pairs (ij) are not all equivalent. In this case, (3.35) becomes

$$-\beta F_{(2)} = N(1-z)\ln\Phi + \frac{Nz}{2}\sum_{k} a_k \ln\sum_{l=1}^{9} e^{-\beta\nu_l(k)} , \tag{3.37}$$

where the sum on k is over the nonequivalent pairs (ij) and a_k gives the weight of each.

D. Three-Spin Cluster Approximation

There are two types of clusters which contribute to $-\beta F'$ in the three-spin cluster approximation. They have been discussed by SCH, and consist of triangles and V-linked diagrams. Using (3.21) and (3.22), one finds that the contribution of the triangles to $-\beta F'$ is

$$\sum_{(ijk)} \{\ln\langle\exp[-2\beta(Q'_{ij}+Q'_{jk}+Q'_{ki}]\rangle - \ln\langle\exp[-2\beta(Q'_{ij}+Q'_{jk})]\rangle - \ln\langle\exp[-2\beta(Q'_{jk}+Q'_{ki})]\rangle - \ln\langle\exp[-2\beta(Q'_{ki}+Q'_{ij})]\rangle + \ln\langle\exp(-2\beta Q'_{ij})\rangle + \ln\langle\exp(-2\beta Q'_{jk})\rangle + \ln\langle\exp(-2\beta Q'_{ki})\rangle\} , \tag{3.38}$$

where the summation is over all sets (ijk). The contribution of the V-linked diagrams is

$$\sum_{(ijk)} \{\ln\langle\exp[-2\beta(Q'_{ij}+Q'_{jk})]\rangle - \ln\langle\exp[-2\beta(Q'_{jk}+Q'_{ki})]\rangle - \ln\langle\exp[-2\beta(Q'_{ki}+Q'_{ij})]\rangle - 2\ln\langle\exp(-2\beta Q'_{ij})\rangle + \ln\langle\exp(-2\beta Q'_{jk})\rangle + \ln\langle\exp(-2\beta Q'_{ki})\rangle\} . \tag{3.39}$$

Therefore the contribution to $-\beta F'$ by three-spin clusters (ijk) is

$$-\beta F'_{(3)} = \sum_{(ijk)} -\beta F'_{\{ijk\}} , \tag{3.40}$$

where

$$-\beta F'_{\{ijk\}} = \ln\langle\exp[-2\beta(Q'_{ij}+Q'_{jk}+Q'_{ki})]\rangle - \ln\langle\exp(-2\beta Q'_{ij})\rangle - \ln\langle\exp(-2\beta Q'_{jk})\rangle - \ln\langle\exp(-2\beta Q'_{ki})\rangle . \tag{3.41}$$

Assuming nearest-neighbor interactions only, for which

$$\Gamma_{ij} = \begin{cases} \Gamma & \text{if } ij \text{ are nearest neighbors} \\ 0 & \text{otherwise,} \end{cases} \tag{3.42}$$

it is found that only two types of triplets contribute to $-\beta F'_{(3)}$. In that case,

$$-\beta F'_{(3)} = \sum'_{(ijk)} -\beta F_{\{ijk\}}(\Delta) + \sum''_{(ijk)} -\beta F_{\{ijk\}}(V) , \tag{3.43}$$

where the primed summation is over all sets (ijk) such that i, j, and k are all nearest neighbors, and the double-primed summation is over all sets $\{ijk\}$ such that i, k are nearest neighbors of j, but not of each other. For the second sum $-\beta F'_{\{ijk\}}$ is found by setting $Q'_{ki} = 0$ in (3.41).

The terms $\ln\langle\exp(-2\beta Q'_{ij})\rangle$ in (3.41) have been evaluated in Sec. III C. The term

$$\ln\langle\exp[-2\beta(Q'_{ij}+Q'_{jk}+Q'_{ki})]\rangle = \ln \mathrm{Tr} e^{-\beta H_0}\exp[-2\beta(Q'_{ij}+Q'_{jk}+Q'_{ki})] + \beta F_0 . \tag{3.44}$$

As in Sec. III C, one defines V by

$$\exp\{-\beta[H_0+2(Q_{ij}+Q_{jk}+Q_{ki})]\}=e^{-\beta H_0}e^{-\beta V}, \tag{3.45}$$

and uses the theorem of Blinc and Svetina[37] to write

$$V=2(Q_{ij}+Q_{jk}+Q_{ki})+(\beta/2!)[H_0,2(Q_{ij}+Q_{jk}+Q_{ki})]$$
$$+(\beta^2/3!)[H_0,[H_0,2(Q_{ij}+Q_{jk}+Q_{ki})]]+\cdots . \tag{3.46}$$

However, use of (3.19) shows that

$$V=2(Q'_{ij}+Q'_{jk}+Q'_{ki}) . \tag{3.47}$$

Therefore, using (3.11) one has

$$e^{-\beta H_0}\exp[-2\beta(Q'_{ij}+Q'_{jk}+Q'_{ki})]$$
$$=\exp\{-\beta(H_0+2[Q_{ij}+Q_{jk}+Q_{ki}])\} . \tag{3.48}$$

Evaluating the exponent as in Sec. III C, one finds

$$\ln\langle\exp[-2\beta(Q'_{ij}+Q'_{jk}+Q'_{ki})]\rangle=-2\beta(\gamma^{00}_{ij}+\gamma^{00}_{jk}+\gamma^{00}_{ki})\overline{O}^2$$
$$-3\ln\Phi+\ln\sum_{l=1}^{27}e^{-\beta\nu'_l(ijk)} . \tag{3.49}$$

Here the $\nu'_l(ijk)$ are the eigenvalues of

$$H'_3(ijk)=-(\tfrac{1}{2}\xi+2\gamma^{00}_{ij}\overline{O})(O^0_i+O^0_j)-(\tfrac{1}{2}\xi+2\gamma^{00}_{jk}\overline{O})$$
$$\times(O^0_j+O^0_k)-(\tfrac{1}{2}\xi+2\gamma^{00}_{ki})(O^0_k+O^0_i)$$
$$+2\sum_{mn}(\gamma^{mn}_{ij}O^m_iO^n_j+\gamma^{mn}_{jk}O^m_jO^n_k+\gamma^{mn}_{ki}O^m_kO^n_i) . \tag{3.50}$$

Using (3.33) and (3.49), (3.41) becomes, for the case where ijk are all nearest neighbors,

$$-\beta F'_{\{ijk\}}(\Delta)=3\ln\Phi+\ln\sum_{l=1}^{27}e^{-\beta\nu'_l(ijk)}-\ln\sum_{l=1}^{9}e^{-\beta\nu_l(ij)}$$
$$-\ln\sum_{l=1}^{9}e^{-\beta\nu_l(jk)}-\ln\sum_{l=1}^{9}e^{-\beta\nu_l(ki)} . \tag{3.51}$$

For the clusters where i and k are nearest neighbors of j, but not of each other, (3.41) becomes

$$-\beta F'_{\{ijk\}}(V)=\ln\langle\exp[-2\beta(Q'_{ij}+Q'_{jk})]\rangle$$
$$-\ln\langle\exp(-2\beta Q'_{ij})\rangle-\ln\langle\exp(-2\beta Q'_{jk})\rangle . \tag{3.52}$$

This is simply (3.41) with $Q'_{ki}=0$. As a result, one can immediately write

$$\ln\langle\exp[-2\beta(Q'_{ij}+Q'_{jk})]\rangle=-2\beta(\gamma^{00}_{ij}+\gamma^{00}_{jk})\overline{O}^2$$
$$-3\ln\Phi+\ln\sum_{l=1}^{27}e^{-\beta\nu''_l(ijk)} , \tag{3.53}$$

where the $\nu''_l(ijk)$ are the eigenvalues of

$$H''_3(ijk)=-(\tfrac{1}{2}\xi+2\gamma^{00}_{ij}\overline{O})(O^0_i+O^0_j)-(\tfrac{1}{2}\xi+2\gamma^{00}_{jk}\overline{O})$$
$$\times(O^0_j+O^0_k)-(\tfrac{1}{2}\xi)(O^0_k+O^0_i)$$
$$+\sum_{mn}(\gamma^{mn}_{ij}O^m_iO^n_j+\gamma^{mn}_{jk}O^m_jO^n_k) . \tag{3.54}$$

Therefore, (3.52) is

$$-\beta F'_{\{ijk\}}(V)=\ln\Phi+\ln\sum_{l=1}^{27}e^{-\beta\nu''_l(ijk)}$$
$$-\ln\sum_{l=1}^{9}e^{-\beta\nu_l(ij)}-\ln\sum_{l=1}^{9}e^{-\beta\nu_l(jk)} . \tag{3.55}$$

The total three-spin cluster approximation to the free energy is

$$-\beta F_{(3)}=-\beta F_0-\beta F'_{(2)}-\beta F'_{(3)} . \tag{3.56}$$

Using (3.35), (3.43), (3.51), and (3.55), collecting terms, and performing the indicated sums, (3.56) becomes

$$-\beta F_{(3)}=\frac{N}{2}(z-1)(z-2)\ln\Phi$$
$$+\frac{Nz}{2}(z_1-2z+3)\sum_k a_k\ln\sum_{l=1}^{9}e^{-\beta\nu_l(k)}$$
$$+\frac{Nz}{2}(z-z_1-1)\sum_m b_m\ln\sum_{l=1}^{27}e^{-\beta\nu'_l(m)}$$
$$+\frac{Nzz_1}{3!}\sum_n c_n\ln\sum_{l=1}^{}e^{-\beta\nu'_l(n)} . \tag{3.57}$$

Here z_1 is the number of nearest neighbors which two nearest neighbors have in common. If all pairs $(n=i,j)$, V-linked diagrams ($m=i,j,k$ with i,k being nearest neighbors of j, but not of each other), and triangles ($n=i,j,k$ with i,j,k all being nearest neighbors) are equivalent, there is only one term in each of $\sum_k$, $\sum_m$, $\sum_n$ and $a_1=b_1=c_1=1$. However, in general, there are several nonequivalent sets of each type of cluster and then $\sum_k$, $\sum_m$, $\sum_n$ are over all nonequivalent clusters, with a_k, b_m, c_n giving the weight of the k, m, and nth clusters, respectively. In particular, for the $Pa3$ lattice all pairs (ij) are equivalent, so $\sum_k a_k=1$; there are two nonequivalent triangles, and seven nonequivalent V-linked diagrams. The weights a_k, b_m, c_n are listed in Tables III, IV, and V, respectively, for both the $Pa3$ and $Pca2_1$ structures. [Note that for magnetism, all pairs, triangles, and V-linked diagrams are equivalent and in this case, (3.57) reduces to Eq. (65) of SCH.]

IV. CALCULATIONS

In the numerical calculations, an arbitrary parameter η was put into $H_2(ij)$ so the model could be varied from an Ising ($\eta=0$) type to a Heisenberg ($\eta=1$) type with η measuring the amount of the off-diagonal EQQ interaction in the Hamiltonian. With the insertion of this parameter, (3.32) takes the form

$$H_2(ij)=2\{[\gamma(0)-2\gamma^{00}_{ij}]\overline{O}(O^0_i+O^0_j)$$
$$+\eta\sum_{mn}\gamma^{mn}_{ij}O^m_iO^n_j\} . \tag{4.1}$$

TABLE III. Representative two-spin clusters and their weights for the fcc and hcp lattices. Molecules i and j are nearest neighbors, $\vec{\Omega}_{ij} = (\theta_{ij}, \phi_{ij})$ are the polar angles specifying the direction of $\vec{R}_{ij}$. For the $Pca2_1$ lattice, $|\vec{R}_{ij}| = r$ for molecules in different hexagonal planes, and $|\vec{R}_{ij}| = a$ for molecules in the same hexagonal plane when $c/a \neq (8/3)^{1/2}$.

Sublattice i	Sublattice j	θ_{ij}	ϕ_{ij}	Weight
		$Pa3$		
1	2	$\pi/2$	$\pi/4$	1
		$Pca2_1$		
1	1	$\pi/2$	0	2/12
1	2	$\pi/2$	$\pi/3$	4/12
1	3	$\cos^{-1}(c/2r)$	$\pi/2$	2/12
1	4	$\cos^{-1}(c/2r)$	$7\pi/6$	2/12
1	4	$\cos^{-1}(c/2r)$	$11\pi/6$	2/12

The calculation of the two-spin cluster approximation for a given value of η involves the following steps: (a) Select a reasonable range of values of the parameter $\bar{O}$. An estimate of this range is given by the limits on $\bar{O}$ in the molecular-field case where $\bar{O} = \langle O_i^0 \rangle$. (b) Pick a set of trial values of $\bar{O}$; diagonalize the fcc and hcp two-spin Hamiltonians and calculate the respective free energies. (c) Approximating $-\beta F_{(2)}$ as a quadratic in $\bar{O}$ at its absolute minima, use the two values of $-\beta F_{(2)}$ next to the lowest calculated value of $-\beta F_{(2)}$ to calculate a minimum, then invert to find the corresponding value of $\bar{O}$. (d) Minimizing $F_{(2)}$ with respect to $\bar{O}$ shows that the best value of $\bar{O}$ is determined by the solution of

$$\mathrm{Tr}\rho_0 O_i^0 = \mathrm{Tr}\tfrac{1}{2}(O_i^0 + O_j^0)\rho_2(ij) . \qquad (4.2)$$

However, in this calculation, the best value of $\bar{O}$ has been determined by minimizing $F_{(2)}$ numerically. Therefore it can be used in (4.2) to obtain a value of the long-range order parameter $\bar{n} = \frac{1}{2}(1 + \frac{1}{3}\langle O_i^0 \rangle)$ within the two-spin cluster approximation.

(e) Repeat steps (a)–(d) for other temperatures.
(f) Values of $\Delta c/a$ ranging from 10^{-4} to 0.1 were inserted and the calculations redone to examine the effects of varying the intermolecular distances and angles on the hcp free energy. The variation of $\Delta c/a$ entered only into the calculation of $\gamma_{ij}^{mn}(\vec{\Omega}_{ij})$.

The same procedures are used in the calculating three-spin cluster approximation to the orientational free energy.

V. RESULTS

A. Two-Spin Cluster Approximation

The results for the long-range order parameter $\bar{n}$ for the two-spin approximation are shown in Figs. 3 and 4. For $\eta = 0$, the first-order transition predicted by molecular-field treatments does not occur. However, $\bar{n}$ does undergo a very rapid transition from a value near one-third to near zero. This transition occurs in a temperature range very close to the first-order transition temperature predicted by molecular-field treatments. As η is increased, the transition becomes sharper in the cubic case and for $\eta \sim 0.8$, one obtains a first-order transition.[35] For the $Pca2_1$ lattice, no phase transition is observed for any value of η. In both cases the temperature for which the molecules start to order decreases with increasing η.

Figures 5 and 6 show the difference between the orientational free energy calculated using (3.36) and (3.37) and the completely orientationally disordered phase, $\Delta F_2 = F_2 + Nk_B T \ln 3$. The Ising models for the $Pa3$ and $Pca2_1$ structures show the correct low-temperature behavior for which $F|_{T=0} = U|_{T=0} = \langle 0|H|0\rangle$. However, for nonzero values of η the two-spin free energy deviates from the correct values at low temperatures. This deviation is larger for the hcp lattice than it is for the fcc lattice, and indicates an overestimation of the importance of short-range order at low temperatures by the two-spin cluster approximation. This also is shown by

TABLE IV. Representative three-spin clusters and their weights for the fcc and hcp lattices. Molecules i, j, and k are all nearest neighbors of each other. $\vec{\Omega}_{ij} = (\theta_{ij}, \phi_{ij})$ are the polar angles specifying direction of intermolecular axes.

Sublattice i	Sublattice j	Sublattice k	θ_{ij}	ϕ_{ij}	θ_{jk}	ϕ_{jk}	θ_{ki}	ϕ_{ki}	Weight
					$Pa3$				
1	2	3	$\pi/4$	π	$\pi/2$	$\pi/4$	$3\pi/4$	$3\pi/2$	18/24
1	2	4	$\pi/4$	0	$3\pi/4$	$3\pi/2$	$\pi/2$	$3\pi/4$	6/24
					$Pca2_1$				
1	1	2	$\pi/2$	0	$\pi/2$	$2\pi/3$	$\pi/2$	$4\pi/3$	6/24
1	1	4	$\pi/2$	0	$\cos^{-1}(+c/2r)$	$7\pi/6$	$\cos^{-1}(-c/2r)$	$5\pi/6$	3/24
1	1	4	$\pi/2$	0	$\cos^{-1}(-c/2r)$	$7\pi/6$	$\cos^{-1}(+c/2r)$	$5\pi/6$	3/24
1	2	3	$\pi/2$	$\pi/3$	$\cos^{-1}(+c/2r)$	$7\pi/6$	$\cos^{-1}(-c/2r)$	$3\pi/2$	3/24
1	2	3	$\pi/2$	$\pi/3$	$\cos^{-1}(-c/2r)$	$7\pi/6$	$\cos^{-1}(+c/2r)$	$3\pi/2$	3/24
1	2	3	$\pi/2$	$2\pi/3$	$\cos^{-1}(+c/2r)$	$11\pi/6$	$\cos^{-1}(-c/2r)$	$3\pi/2$	3/24
1	2	3	$\pi/2$	$2\pi/3$	$\cos^{-1}(-c/2r)$	$11\pi/6$	$\cos^{-1}(+c/2r)$	$3\pi/2$	3/24

TABLE V. Representative three-spin clusters and their weights for the fcc and hcp lattices. Molecules i and k are nearest neighbors of j, but not of each other. $\vec{\Omega}_{ij} = (\theta_{ij}, \phi_{ij})$ are the polar angles specifying the direction of the intermolecular axis.

	Sublattice						
i	j	k	θ_{ij}	ϕ_{ij}	θ_{jk}	ϕ_{jk}	Weight
				$Pa3$			
1	2	1	$\pi/4$	π	$\pi/4$	0	24/84
1	2	4	$\pi/4$	π	$\pi/4$	$\pi/2$	12/84
1	2	3	$\pi/4$	π	$\pi/2$	$3\pi/4$	12/84
1	2	1	$\pi/4$	π	$\pi/4$	π	6/84
1	2	4	$\pi/4$	π	$\pi/4$	$3\pi/2$	12/84
1	2	1	$\pi/4$	0	$\pi/4$	0	6/84
1	2	4	$\pi/4$	0	$\pi/4$	$3\pi/2$	12/84
				$Pca2_1$			
1	1	2	$\pi/2$	0	$\pi/2$	$5\pi/3$	4/84
1	1	4	$\pi/2$	0	$\cos^{-1}(+c/2r)$	$11\pi/6$	2/84
1	1	4	$\pi/2$	0	$\cos^{-1}(-c/2r)$	$11\pi/6$	2/84
1	1	1	$\pi/2$	0	$\pi/2$	0	2/84
1	1	2	$\pi/2$	0	$\pi/2$	$\pi/3$	4/84
1	1	3	$\pi/2$	0	$\cos^{-1}(+c/2r)$	$\pi/2$	4/84
1	1	3	$\pi/2$	0	$\cos^{-1}(-c/2r)$	$\pi/2$	4/84
1	1	4	$\pi/2$	π	$\cos^{-1}(+c/2r)$	$7\pi/6$	2/84
1	1	4	$\pi/2$	π	$\cos^{-1}(-c/2r)$	$7\pi/6$	2/84
1	2	3	$\pi/2$	$\pi/3$	$\cos^{-1}(+c/2r)$	$11\pi/6$	4/84
1	2	3	$\pi/2$	$\pi/3$	$\cos^{-1}(-c/2r)$	$11\pi/6$	4/84
1	2	1	$\pi/2$	$\pi/3$	$\pi/2$	$\pi/3$	2/84
1	2	4	$\pi/2$	$\pi/3$	$\cos^{-1}(+c/2r)$	$\pi/2$	2/84
1	2	4	$\pi/2$	$\pi/3$	$\cos^{-1}(-c/2r)$	$\pi/2$	2/84
1	2	1	$\pi/2$	$\pi/3$	$\pi/2$	$2\pi/3$	4/84
1	2	4	$\pi/2$	$2\pi/3$	$\cos^{-1}(+c/2r)$	$\pi/2$	2/84
1	2	4	$\pi/2$	$2\pi/3$	$\cos^{-1}(-c/2r)$	$\pi/2$	2/84
1	2	1	$\pi/2$	$2\pi/3$	$\pi/2$	$2\pi/3$	2/84
1	2	3	$\pi/2$	$2\pi/3$	$\cos^{-1}(+c/2r)$	$7\pi/6$	4/84
1	2	3	$\pi/2$	$2\pi/3$	$\cos^{-1}(-c/2r)$	$7\pi/6$	4/84
1	2	3	$\pi/2$	$4\pi/3$	$\cos^{-1}(+c/2r)$	$7\pi/6$	2/84
1	2	3	$\pi/2$	$4\pi/3$	$\cos^{-1}(-c/2r)$	$7\pi/6$	2/84
1	2	3	$\pi/2$	$5\pi/3$	$\cos^{-1}(+c/2r)$	$11\pi/6$	2/84
1	2	3	$\pi/2$	$5\pi/3$	$\cos^{-1}(-c/2r)$	$11\pi/6$	2/84
1	3	2	$\cos^{-1}(+c/2r)$	$\pi/2$	$\cos^{-1}(+c/2r)$	$\pi/6$	2/84
1	3	2	$\cos^{-1}(+c/2r)$	$\pi/2$	$\cos^{-1}(+c/2r)$	$5\pi/6$	2/84
1	3	1	$\cos^{-1}(+c/2r)$	$\pi/2$	$\cos^{-1}(+c/2r)$	$3\pi/2$	2/84
1	3	2	$\cos^{-1}(-c/2r)$	$\pi/2$	$\cos^{-1}(-c/2r)$	$\pi/6$	2/84
1	3	2	$\cos^{-1}(-c/2r)$	$\pi/2$	$\cos^{-1}(-c/2r)$	$5\pi/6$	2/84
1	4	1	$\cos^{-1}(+c/2r)$	$7\pi/6$	$\cos^{-1}(+c/2r)$	$\pi/6$	2/84
1	4	1	$\cos^{-1}(+c/2r)$	$7\pi/6$	$\cos^{-1}(+c/2r)$	$5\pi/6$	2/84
1	4	1	$\cos^{-1}(+c/2r)$	$11\pi/6$	$\cos^{-1}(+c/2r)$	$\pi/6$	2/84
1	4	1	$\cos^{-1}(+c/2r)$	$11\pi/6$	$\cos^{-1}(+c/2r)$	$5\pi/6$	2/84

the fact that the molecules do not order at all for $\eta = 1$.

The Gibbs potential $G = F + V$ is minimized for a phase transition at constant pressure. Crystallographic transition will occur when $\Delta G = G(\text{fcc}) - G(\text{hcp})$. However, $\Delta G = \Delta F + p\Delta V$ and for normal pressures where $p \sim 1$ atm, the term $p\Delta V/Nk_B \leq 7\times10^{-6}$ K and can be neglected for solid o-H_2. Therefore, a comparison of $F(\text{fcc}) - F(\text{hcp})$ is adequate. Figure 7 shows plots of this difference for several values of η. It is seen that a structural transition does occur in the region where the two-spin cluster variation method is valid, that is, for $\eta \leq 0.75$. The hcp phase is favored at high temperatures. One finds $\Delta F/Nk_B T_b \sim 5\times10^{-3}$ for T greater than the fcc-hcp transition temperature, $T_{\text{fcc-hcp}}$. Here T_b is the branching temperature[7] and k_B is Boltzmann's constant. For o-H_2, T_b has a value $19\Gamma/3k_B = 4.91$ K using $\Gamma = 0.539$ cm^{-1}.[30] This gives $\Delta F/Nk_B \sim 2.4\times10^{-2}$ K. An estimate of the difference in the zero-temperature lattice contribution to the free energy also indicates the hcp

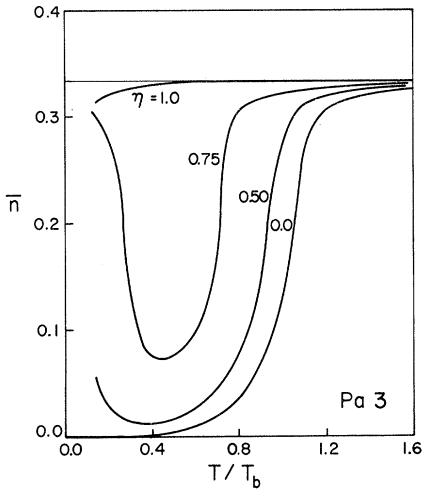

FIG. 3. The long-range order parameter $\bar{n}$ for fcc o-H_2 vs the reduced temperature for several values of the anisotropy parameter η, calculated using the two-spin cluster variation method of SCH. $Pa3$ space group.

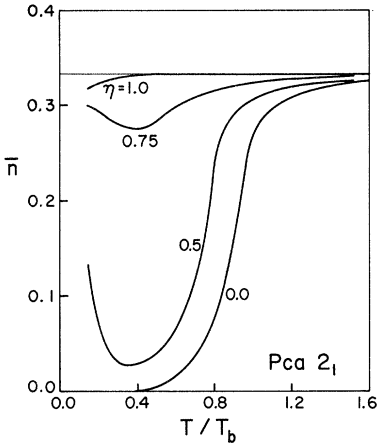

FIG. 4. The long-range order parameter $\bar{n}$ for hcp o-H_2 vs the reduced temperature for several values of the anisotropy parameter η, calculated using the two-spin cluster variation method of SCH. $Pca2_1$ space group.

lattice is favored by about 10^{-3} K over the fcc phase.[21] The above results are for $\Delta c/a = 0$; here $\Delta c/a$ measures the deviation of the c/a ratio from the ideal hcp value of $(8.3)^{1/2}$. With $\Delta c/a \neq 0$, one finds a structural transition even for $\eta = 1.0$. However, it occurs at very low temperatures in the region where the two-spin cluster approximation is not expected to be valid. For deuterium $\Gamma = 0.736$ cm^{-1} from optical data,[30] so that $T_b = 6.71$ K.

B. Three-Spin Cluster Approximation

The three-spin results differ substantially from those of the two-spin approximation. The three-spin calculation was performed only for $\eta = 0.0$ and $\eta = 1.0$ because of the large amounts of computer time required. The $\eta = 0$ results are nearly the same as the corresponding results for the two-spin cluster approximation and will not be presented.

The extrema of the free energy for the fcc and hcp lattices are shown in Figs. 8 and 9. The associated branches of the long-range order parameter for the two lattices are shown in Figs. 10 and 11. Related curves are indicated by similar lettering. Within the three-spin cluster approximation we find two first-order orientational transitions in the fcc and hcp lattices under consideration. However, the details of these transitions are quite different.

In the fcc lattice, at low temperatures the stable solution (labeled A in Fig. 8) is a state for which $\bar{n}$ is nearly zero. This corresponds to ordering along the z axes. As the temperature is increased, $\bar{n}$ increases gradually until T/T_b is between 0.73 and 0.74. A first-order transition then occurs to the state labeled B in Fig. 8. In this state $\bar{n} = 0.5$ at low temperatures, and the molecular axes are ordered in the x and y planes. Since the z axes are along the $[\pm 1, \pm 1, \pm 1]$ directions, these are planes perpendicular to the $[\pm 1, \pm 1, \pm 1]$ axes. In the same temperature region, the solutions labeled D and E appear. Solution E is a relative minima with $\bar{n} \sim \frac{1}{3}$ and is a state with no long-range order. For T/T_b between 0.78 and 0.79, another first-order transition occurs with the system going to the state with no long-range order.

For the hcp system, the molecules also order in the state (labeled A in Fig. 9) with $\bar{n} = 0$ at low tem-

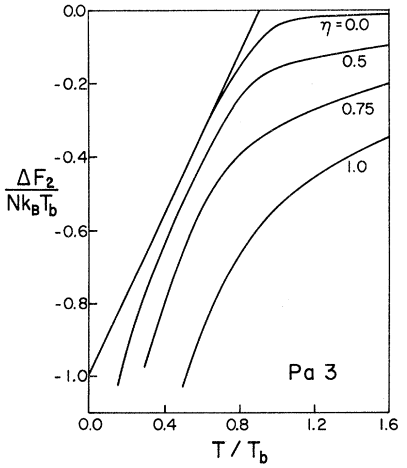

FIG. 5. Contribution of the orientational coupling to the free energy per molecule for fcc o-H_2 within the two-spin cluster approximation. The difference between the free energies of the ordered and disordered phases is shown for several values of η. $Pa3$ space group.

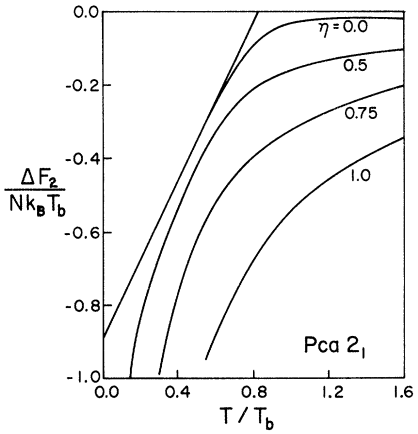

FIG. 6. Contribution of the orientational coupling to the free energy per molecule for the hcp o-H_2 within the two-spin cluster approximation. The difference between the free energies of the ordered and disordered phases is shown for several values of η. $Pca2_1$ space group.

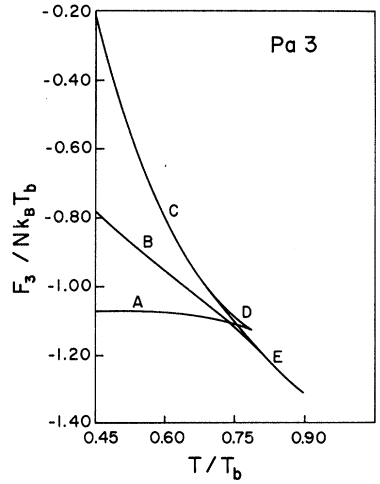

FIG. 8. Free energy for the fcc ($Pa3$) structure showing all branches of the solution. A particular extremum and its corresponding order parameter in Fig. 10 have the same lettering.

peratures. As the temperature rises, $\bar{n}$ increases, but more rapidly than in the cubic case. When T/T_b is between 0.71 and 0.72, this system also undergoes a first-order transition to the state labeled B in which $\bar{n} \sim 0.5$. However, the solution corresponding to $\bar{n} \sim \frac{1}{3}$ or the completely disordered state does not appear. Rather, the order parameter in the ordered state at low temperatures makes a rapid transition from a value near zero to a value near one-third. For T/T_b between 0.80 and 0.81, a first-order transition occurs from the state in which $\bar{n} \sim 0.5$ to the state in which $\bar{n}$ now has a value near one-third.

The difference between the minimum orientational free energy in the three-spin cluster approximation calculated using (3.57) and the completely disordered state is shown in Fig. 12 for the fcc and hcp lattices. The behavior of the free energy is substantially improved by the inclusion of the three-spin clusters. In the low-temperature and high-temperature regions, large amounts of free energy remain indicating the remnants of short-range order imposed on the system by the use of the cluster approximation. As we noted previously,[36] the anomaly in the specific heat near the transition temperature for which $\partial^2 F/\partial T^2 > 0$ indicates deviations of the molecular symmetry axes from the $Pa3$ directions as a result of the increasing importance of the interactions of smaller clusters of molecules at higher temperatures.

The possibility of the quadrupole-quadrupole interaction leading to a structural phase transition

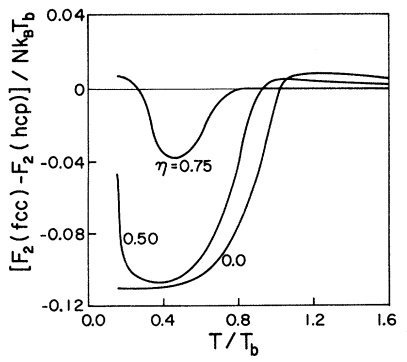

FIG. 7. Comparison of the two-spin approximation to the orientational free energies of fcc and hcp o-H_2 for several values of η.

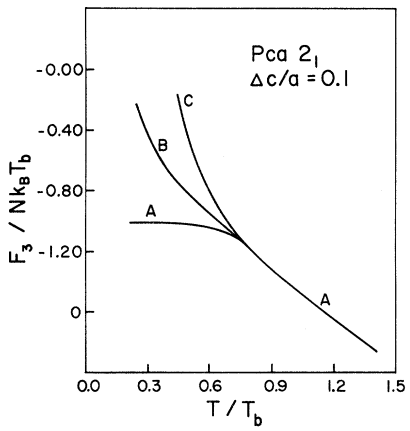

FIG. 9. Free energy for the hcp ($Pca2_1$) structure showing all branches of the solution. A particular extremum and its corresponding order parameter in Fig. 11 have the same lettering.

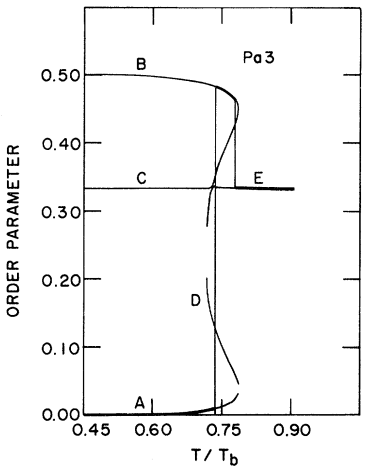

FIG. 10. The long-range order parameter $\bar{n}$ for fcc o-H_2 vs the reduced temperature with the anisotropy parameter $\eta = 1$, calculated using the three-spin cluster variation method of SCH. $Pa3$ space group. The vertical lines mark the first-order transitions.

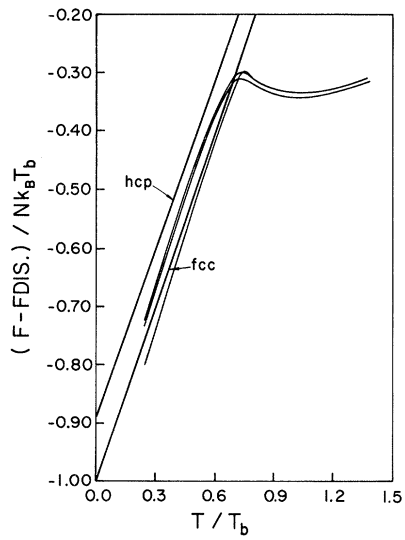

FIG. 12. The difference between the orientational free energy calculated in the three-spin approximation and the completely disordered state for the fcc and hcp lattices. Straight lines represent the energies of the completely ordered states. Energies in the hcp case are shown for $\Delta c/a = 0.0$ and 0.1.

can again be examined by a consideration F(fcc) $-F$(hcp), where F(fcc) and F(hcp) refer to the orientational free energy within the three-spin cluster approximation. For $\eta = 1$ and $\Delta c/a = 0$, the fcc phase is stable at low temperatures. In the region where the molecules order in the plane perpendicular to the $[\pm 1, \pm 1, \pm 1]$ directions, the hcp lattice becomes stable over a small temperature range. The exact transition temperatures cannot be determined from our results. However, examination of the results make it appear that hcp phase becomes stable at about $T/T_b = 0.72$ and then destabilizes at about $T/T_b = 0.77$. For $\Delta c/a \sim 10^{-4}$, the hcp free energy is raised slightly. For $\Delta c/a > 10^{-4}$, and increasing, the hcp free energy drops rapidly until $\Delta c/a$ is slightly larger than 0.01. At this point the hcp phase becomes stable at high temperatures. Figure 13 shows the difference between the fcc and hcp orientational free energies for $\Delta c/a = 0.0$ and 0.1.

Inclusion of the estimated difference between the zero-temperature lattice energies increases the temperature range over which the hcp phase is stable. The transition near $T/T_b = 0.72$ is insensitive to variations in $\Delta c/a$, or changes in the estimate of the zero-temperature lattice contribution to the free energy because the fcc free energy drops rapidly in this region. This transition remains when $\Delta c/a$ or the lattice contribution to the free energy are large enough to make the hcp phase stable at all high temperatures.

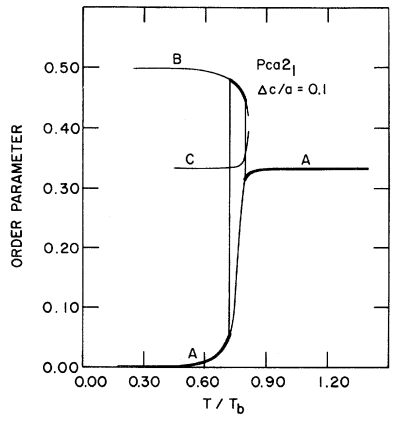

FIG. 11. The long-range order parameter $\bar{n}$ for hcp o-H_2 vs the reduced temperature with the anisotropy parameter $\eta = 1$, calculated using the three-spin cluster variation method of SCH. $Pca2_1$ space energy. The vertical lines mark the first-order transitions.

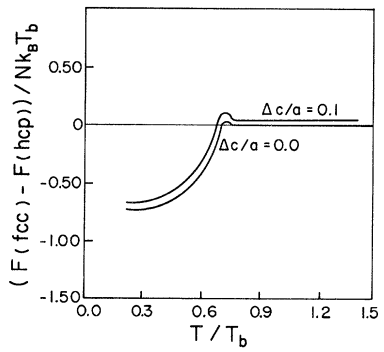

FIG. 13. Comparison of the three-spin approximation to the orientational free energies of fcc and hcp o-H_2. Included are the differences for $\Delta c/a = 0.0$ and 0.1.

VI. CONCLUSIONS

The two- and three-spin cluster approximations have been applied to rigid-lattice models of hcp and fcc o-H_2 molecules interacting via a quadrupole-quadrupole interaction. These approximations lead to significant improvement over previous theories in the transition region because of the inclusion of the two-molecule, three-molecule, etc., correlations as well as the effects of molecules outside the cluster by a variational procedure. However, especially at low temperatures, it overemphasizes the importance of short-range correlations.

Comparison of the order parameters and free energies for $\eta = 1.0$ show that the three-spin cluster approximation gives much better results than the two-spin method. In particular, we find the two-spin order parameter behaves correctly only at higher temperatures, whereas the three-spin order parameter approaches the correct low-temperature limit in agreement with molecular-field and librational-wave treatments.

The first-order orientational transitions observed have not been predicted by other calculations and could be the result of the approximation. It has recently been shown that within the framework of the molecular-field theory the nearest-neighbor approximation can lead to spurious results.[38] Since these transitions occur in the same temperature region as the anomaly in the free energy, it is probable that they are not physically significant. However, the transitions are important insofar as they reflect the instability of the lattices under consideration with respect to space groups with other types of ordering. In this temperature region, the molecular axes show large deviations from the $Pa3$ symmetry directions and the inclusion of further interactions could affect the behavior of the order parameter. The effects of further neighbor interactions are presently under investigation. It may also be that other lattices become stable in this region as has been found in molecular-field studies by James.[38] He performed self-consistent calculations with random initial molecular configurations and found several lattice with free energies close to those of the $Pa3$ and $Pca2_1$ lattices. The present calculations are being performed for those lattices which he found to be stable or nearly stable using the molecular-field approximation. Preliminary indications are that the $P2_1/c$ space group has a lower orientational energy than either the $Pa3$ or $Pca2_1$ structures at high temperatures.[39] Consideration of this space group removes a substantial portion of the anomalous behavior of the free energy. Inclusion of other lattices may remove the remaining portion.

It has been suggested from experimental evidence that the molecules begin to order in the hcp phase, then this structural transition occurs and aids in the ordering.[19] Our results could be interpreted in that manner since the free energy of the stable solution $\bar{n} \sim 0.5$ is not much lower than the disordered solution, and hence the disordered solution might be made stable by the presence of defects. The molecules would then start to order in the hcp phase with the structural transition occurring when the molecules would be more aligned in the fcc phase than in the hcp phase. From a comparison of the order parameters, we see this would happen at about $T/T_b = 0.75$, or $T \cong 3.68$ K which is much closer to the predicted structural transition at about 2.8 K for orthohydrogen[31,32] than previous treatments. For deuterium the $0.75T_b$ is 5.03 K and the extrapolated transition temperature from experiment is about 4 K.[32]

The temperature range over which the hcp lattice is stable for $\Delta c/a = 0$ seems to be closely related to the occurrence of orientational transitions. This may be a further indication that other hcp space groups could be significant. It is also possible that a distortion of the hcp lattice is suggested since pure quadrupole-quadrupole interactions cause the rigid hcp lattice to remain stable at high temperatures only for nonzero values of $\Delta c/a$. Although a distortion has not been observed experimentally, a small distortion has previously been predicted by Van Kranendonk,[40] due to translation-libration interaction. We find a $\Delta c/a$ somewhat larger than 0.01 causes the $Pca2_1$ space group to be favored at high temperatures. The exact value was not found because of the large amount of time involved. This value of $\Delta c/a$ would probably be reduced if the effects of a nonrigid lattice were included.

In summary, we conclude that the quadrupole-quadrupole interactions can lead to a structural phase transition from a fcc ($Pa3$) lattice at low temperatures to a hcp ($Pca2_1$) lattice at high temperatures. The predicted transition temperature is about 1 K higher than the extrapolated experimental transition temperature of 2.8 K. For ortho-para mixtures, this transition temperature is a function of the para concentration.[31] A cluster expansion for ortho-para mixtures would be indicated, this calculation is being done. In addition, the effects of the lattice have only been estimated, and the combined effects of the transitional and librational motions of the molecules should be considered for a complete description of the properties of solid hydrogen and deuterium as a function of temperature. Work on these problems is in progress.

†Work supported by NSF Grant No. 22553.

*Permanent address.

‡Work performed in part in the Ames Laboratory of the U. S. Atomic Energy Commission. Contribution No. 3088.

[1]J. C. Raich and H. M. James, Phys. Rev. Letters 16, 173 (1966).
[2]H. M. James and J. C. Raich, Phys. Rev. 162, 649 (1967).
[3]J. C. Raich and R. D. Etters, Phys. Rev. 155, 457 (1967).
[4]H. M. James, Phys. Rev. 167, 862 (1968).
[5]S. Homma, K. Okada, and H. Matsuda, Progr. Theoret. Phys. (Kyoto) 36, 1310 (1966); 38, 767 (1967).
[6]H. Ueyama and T. Matsubara, Progr. Theoret. Phys. (Kyoto) 38, 784 (1967).
[7]J. C. Raich and R. D. Etter, Phys. Rev. 168, 425 (1968).
[8]F. G. Mertens, W. Biem, and H. Hahn, Z. Physik 213, 33 (1968); 220, 1 (1969).
[9]C. F. Coll and A. B. Harris, Phys. Rev. B 2, 1176 (1970).
[10]C. F. Coll, III, A. B. Harris, and A. J. Berlinsky, Phys. Rev. Letters 25, 858 (1970).
[11]A. B. Harris, Phys. Rev. B 1, 1881 (1970).
[12]A. B. Harris, Phys. Rev. B 2, 3495 (1970).
[13]J. C. Raich and R. D. Etters, J. Phys. Chem. Solids 29, 1561 (1968).
[14]A. B. Harris, Solid State Commun. 6, 149 (1968).
[15]J. C. Raich and R. D. Etters, Nuovo Cimento 57B, 224 (1968).
[16]T. Nakamura, Progr. Theoret. Phys. (Kyoto) 14, 135 (1955).
[17]A. J. Berlinsky and A. B. Harris, Phys. Rev. A 1, 878 (1970).
[18]R. L. Mills and A. F. Schuch, Phys. Rev. Letters 15, 722 (1965).
[19]A. F. Schuch, R. L. Mills, and D. A. Depatie, Phys. Rev. 165, 1302 (1968).
[20]K. F. Mucker, S. Talhouk, P. M. Harris, D. White, and R. A. Erickson, Phys. Rev. Letters 15, 586 (1965); 16, 799 (1966).
[21]L. N. Nosanow (private communication to J. C. Raich).
[22]J. C. Raich and R. D. Etters, J. Chem. Phys. 55, 3901 (1971).
[23]F. G. Mertens (unpublished).
[24]B. Strieb, H. B. Callen, and G. Horwitz, Phys. Rev. 130, 1798 (1963).
[25]H. P. Gush and J. Van Kramendonk, Can. J. Phys. 40, 1461 (1962).
[26]M. E. Rose, *Elementary Theory of Angular Momentum* (Wiley, New York, 1957).
[27]O. Nagai and T. Nakamura, Progr. Theoret. Phys. (Kyoto) 24, 432 (1960); 30, 412 (1963).
[28]J. Felsteiner, Phys. Rev. Letters 15, 1025 (1965).
[29]M. Clouter and H. P. Gush, Phys. Rev. Letters 15, 200 (1965).
[30]W. N. Hardy, I. F. Silvera, and J. P. McTague, Phys. Rev. Letters 22, 297 (1969); 26, 127 (1971).
[31]J. F. Jarvis, D. Ramm, H. Meyer, and R. L. Mills, Phys. Letters 25A, 692 (1967).
[32]D. Ramm, H. Meyer, and R. L. Mills, Phys. Rev. B 1, 2763 (1970).
[33]H. Miyagi and T. Nakamura, Progr. Theoret. Phys. (Kyoto) 37, 641 (1967).
[34]H. M. James, Phys. Rev. 167, 167 (1968).
[35]J. C. Raich and R. D. Etters, Solid State Commun. 7, 1031 (1969).
[36]R. J. Lee, J. C. Raich, and R. D. Etters, Solid State Commun. 8, 1803 (1970).
[37]R. Blinc and S. Svertina, Phys. Rev. 147, 423 (1966).
[38]H. M. James, Phys. Rev. Letters 24, 815 (1970).
[39]R. J. Lee and J. C. Raich, Phys. Rev. Letters 27, 1137 (1971).
[40]J. Van Kranendonk and V. F. Sears, Can. J. Phys. 44, 313 (1966).

PHYSICAL REVIEW B VOLUME 5, NUMBER 4 15 FEBRUARY 1972

Infrared Absorption by Impurity-Pair Resonant Modes in NaCl : F†

C. R. Becker
Physikalisches Institut der Universität, 8700 *Würzburg*, *Germany*
and
T. P. Martin
Max-Planck-Institut für Festkörperforschung, 7000 *Stuttgart*, *Germany*
(Received 17 September 1971)

New resonant-mode infrared absorption lines have been observed in NaCl with high concentrations of fluorine impurities. The quadratic concentration dependence of the strength of these lines indicates that they are due to pairs of fluorine impurities. At the resonant frequencies, the motion of some host ions appears to be as important as the motion of the impurities themselves.

INTRODUCTION

Many impurities in alkali halides induce an easily observed far-infrared absorption with concentrations of only 0.1 mole%. Essentially all this absorption can be attributed to isolated impurity ions at substitutional sites in the host lattice. However, a 1-mole% concentration of impurities should result in impurity-pair absorption comparable to the total absorption at 0.1 mole%. In general, this impurity-pair absorption would be difficult to observe above the isolated impurity absorption background. However, if the impurity pairs give rise to resonant or localized modes, ob-